

MODELING AND SIMULATION OF A COPPER ELECTROLYSIS CELL GROUP

Ilkka S. Laitinen¹, Juha T. Tantt¹

¹Tampere University of Technology, Department of Information Technology
P.O. Box 300, FIN-28101 Pori, Finland

ilkka.laitinen@tut.fi (Ilkka Laitinen)

Abstract

Increasing demands for energy efficiency and high quality of products advice to use computer aided modeling, simulation and optimization in product development. In this paper the modeling of the copper electrolysis is in the focus. The energy consumption of the copper electrolysis is high. Electrical disturbances – like contact failures and short circuits – even increase the energy consumption and also decrease the quality of produced copper. To gain better understanding and to be able to improve the process a computationally feasible and reliable model of copper electrolysis cell group is of great importance. In this paper a multiphysical FEM model of copper electrolysis cell group is presented. Due to the high complexity of the cell group geometry and physical phenomena, several simplifications and approximations are necessary in order to make the model computationally feasible. A number of simplifications are proposed. Simulation results depend substantially on disturbance location in the cell group. A statistical approach is proposed such that different cell group designs could be compared regardless the disturbance location.

Keywords: FEM, modeling, simulation, copper electrolysis.

Presenting Author's Biography

Juha T. Tantt was born in Tampere, Finland, on November 25, 1957. He obtained his M.Sc. and Doctor of Technology (Ph.D.) degrees in Electrical Engineering from Tampere University of Technology in 1980 and 1987, respectively. From 1984 to 1992 he held various teaching and research positions at the Control Engineering Laboratory of Tampere University of Technology. He currently holds professorship of Information Technology at Tampere University of Technology, Pori. His research interests are mathematical modeling of dynamic systems and applications of signal processing in bioacoustics.



1 Introduction

The copper electrolysis process is used to produce pure copper in industrial scale in large electrolysis cell groups. Pure copper is needed for example in conductors, where even small amounts of impurities decreases the electrical conductivity. As mentioned in [1, p. 280]: *“The principal technical objective of the refinery is to produce high-purity cathode copper. Other important objectives are to produce this pure copper rapidly and with minimum consumption of energy and manpower”*. The energy consumption of copper electrolysis is high. Electrical disturbances, like loose electrode busbar contacts and short circuits between electrodes, can increase the energy consumption and decrease the amount and quality of produced copper thus reducing its market value. It can be argued that the current distribution uniformness on the electrolysis cell group affects greatly on objectives of copper electrolysis [2, p. 852][3]. The intercell busbar (ICBB) system is used to connect electrolysis cells electrically in series, and it has a significant effect to the current distribution. Thus maintaining current density uniformity is one of the main objectives in the design of an ICBB system.

Computationally feasible and accurate model might offer significant advantages in design process of copper electrolysis cell group. Copper electrolysis cells have been modeled in the past by using resistance networks [4, p. 148]. A resistance network model of the cell group has several advantages. Most importantly, it is simple and its solution is easy to compute. However, it is only a rough approximation of the electrical system. In addition, it is difficult to model multiphysical phenomena using resistance networks.

Due to the limitations of the resistance network models, the FEM approach is used for modeling an electrolysis cell group. An accurate model of the electrolysis process is multiphysical: it includes current distributions and the thermal effect caused by resistive heating. Our model includes these multiphysical phenomena and allows simulation of different electrolysis processes with arbitrary cathode constructions and ICBB systems. Our main goal was to model the current distribution within the cell group. Phenomena assumed to have little affect on the current distribution, were not modeled (e.g. chemical reactions, fluid motion).

In large FEM-models it is often necessary to make simplifications and approximations, since the solution time is typically a polynomial function of the number of degrees of freedom (DOF). There are several ways to reduce the number of DOF: simplification of geometry, by taking advantage of model symmetry, avoiding small details in geometry, using suitable mesh elements and element basis functions. In our model shell elements are used exclusively. The use of shell elements is reasonable for flat geometries like electrode plates, since dependent variables – the electric potential and the temperature – are homogeneous in the direction to be ignored. The shell element modeling requires considerable modifications to the equations and material constants [5].

The modeling aspects of a single electrolysis cell are presented first time in [5] together with verification of modeling accuracy. The model in [5] includes 31 anodes and 30 cathodes, busbars, the electrolyte and an optional short circuit. Some simulation results of copper electrolysis cell group containing seven electrolysis cells are presented in [3]. In this paper a FEM model of an electrolysis cell group is presented including an empirical model of electrode busbar contact. The effective currents are introduced for measuring the current distribution uniformity in the electrolysis process. Moreover, the change in disturbance location can affect significantly the performance of the cell group. This raises two obvious questions: (i) How much the performance is affected and (ii) how to eliminate the effect of disturbance location so that different cell group designs could be compared regardless of disturbance location. To answer the question (i), simulation of the electrolysis cell group model over all disturbance locations is performed. In addition, the disturbance location probability distribution is assumed to provide an answer to question (ii). Then these results are used to demonstrate the effects of the ICBB splitting to the performance of the cell group.

A short overview of the copper electrolysis process is given in section 2. In section 3 the model geometry is presented and issues concerning the meshing are discussed. Also, the modeling approximations are discussed and some essential modeling equations presented in section 3. In section 4 the effects of disturbance location are presented and the ICBB systems compared using the statistical approach. Finally, in section 5, conclusions are presented.

2 The copper electrolysis process

Depending on the type of copper ore, pyrometallurgical or hydrometallurgical process is used to produce pure copper from copper ore. The electrorefining (ER) is part of the pyrometallurgical process. In the ER process pure copper is deposited from the raw copper anode to the cathode by using direct current. The electrowinning (EW) is part of the hydrometallurgical process. In the EW process copper ions are depleted from electrolyte to the cathode by using inert anodes and direct current. [1, Chapters 1,16,19]

The industrial scale EW process takes place in large, 4-9 m long electrolysis cells [1, Sec. 19]. A large electrolysis cell group consist of individual electrolysis cells, which are connected electrically in series by the ICBB system. An overview to a modern EW facility is shown in Fig. 1.

2.1 The Intercell Busbar Systems

Several ICBB systems are available for industrial scale copper electrolysis. The Walker system [6] was invented in 1901, and it is based on electrical connection of adjacent cell electrodes by parallel connection (see Fig. 2). The Whitehead intercell busbar system [7], patented in 1916, in contrast to the Walker system, is based on electrical connection of adjacent cell elec-



Fig. 1 An overview to the modern electrowinning facility

trodes by serial connection (see Fig. 3). This arrangement causes electrical current to be injected directly from a cathode to an anode in the next cell. Modern busbar systems, the Outotec DoubleContact™ [8, 9, 10] and Optibar Segmented Intercell Busbar System [4] can be seen as modifications and extensions to Walker or Whitehead systems.

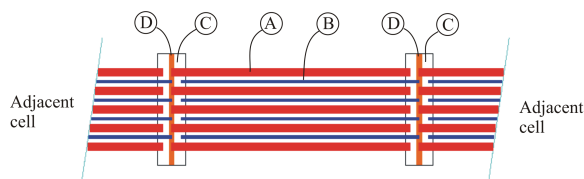


Fig. 2 Top view of the Walker System consisting of the anodes (A), the cathodes (B), the insulator (C) and the intercell busbar (D) [11, p. 304]

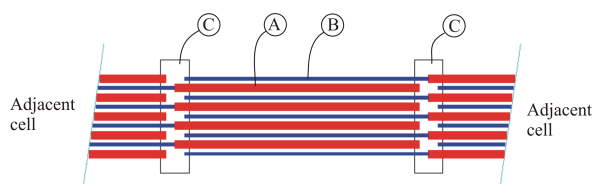


Fig. 3 Top view of the Whitehead system consisting of the anodes (A), the cathodes (B) and the insulator (C) [11, p. 304]

For the ER process the cell voltage is about 0.3 V and the cathodic current density is 260 – 340 A/m² [1, p. 274-275]. Accordingly, for the EW process the cell voltage is about 2 V and the cathodic current density is 150 – 340 A/m² [1, p. 332-333]. The energy consumption in copper electrolysis is high. Typically, producing a ton of copper requires 300 – 400 kWh in the ER and 2000 kWh in the EW process [1, p. 328]. Electrical disturbances like stray currents, contact failures and short circuits increase the energy consumption and decrease

the quality of produced cathode copper. In the contact failure the contact resistance between the electrode and busbar is increased due to oxidation or dirt. As a result the cell voltage increases. The short circuit develops between the anode and cathode due to locally increased cathodic current density or nonuniform cathode copper deposition.

According to Faraday's law of electrolysis, the theoretical mass \hat{m} (kg) of produced substance at an electrode is

$$\hat{m} = \frac{M}{zF} Q = \zeta Q, \quad (1)$$

where $\zeta = M(zF)^{-1}$ is a constant (kg/C), Q is the electric charge (As), M is the molar mass of substance (kg/mol), z is the valence number of the substance as an ion in solution (electrons per ion) and F is the Faraday's constant (96485.3383 C/mol). The electric charge is given by $Q = \int_0^T I(t) dt$, where $I(t)$ is the electric current, t is the time and T is the duration of the electrolysis. [12]

Constants in Eq. (1) for the copper electrolysis are $M = 63.546 \cdot 10^{-3}$ and $z = 2$. Thus the theoretical mass \hat{m}_{cu} of the produced cathode copper is

$$\hat{m}_{\text{cu}} = \zeta_{\text{cu}} Q = 3.2930 \cdot 10^{-7} \frac{\text{kg}}{\text{C}} Q. \quad (2)$$

The performance of copper electrolysis process is measured by current distribution uniformity, current efficiency and specific energy consumption. The current efficiency η_I of copper electrolysis process is defined as

$$\eta_I = \frac{m_{\text{cu}}}{\hat{m}_{\text{cu}}}, \quad (3)$$

where m_{cu} is the mass of produced cathode copper. Accordingly, the specific energy consumption E_s (J/kg) is defined as

$$E_s = \frac{E_e}{m_{\text{cu}}}, \quad (4)$$

where E_e is the electrical energy (J) consumed in the copper electrolysis process.

3 The FEM modeling of the electrolysis cell group

The COMSOL Multiphysics™ [13] is used in modeling the electrolysis cell group. The Comsol Multiphysics™ easily allows coupling of several physical phenomena to model multiphysical phenomena such as resistive heating. In addition, it includes a number of predefined application modes making the modeling in most cases an easy task. In this paper the weak form modeling is used to define the equation system to the model. The weak form modeling requires the weak form of the equations, including PDE's. See [14, p. 60] for mathematical weak form and [15, p. 253] for weak form used for building COMSOL models.

The main issues in modeling the electrolysis cell group are: (i) the geometry is large, (ii) the geometry contains

thin subgeometries like electrode plates, (iii) the electrolysis process contains stochastic parts and (iv) the process is time dependent. Stochastic parts of the process include electrode busbar contact resistance, non-uniform growth of deposited copper and inaccuracy in electrode positioning. Solutions to issues (i) and (ii) are discussed in section 3.1. Stochastic parts (iii) of the process are neglected or approximated by deterministic models as described in section 3.2. Time dependency (iv) of the process is neglected and a stationary model is used. The use of shell elements causes changes in the modeling equations and requires approximations in expressing physical properties of composite structures. These are discussed in subsections 3.3 and 3.4.

3.1 The model geometry and meshing

The single electrolysis cell model presented in [5] has a geometry as depicted in Fig. 4. The geometry includes the anodes (A), the cathodes (B), the electrolyte (C), the anode busbar (D), the anode voltage equalizing bar (E), the cathode busbar (F) and the cathode voltage equalizing bar (G). The electrolyte and the short circuit (not shown in Fig. 4) are modeled as a solid, the other components are modeled as shell elements. The sin-

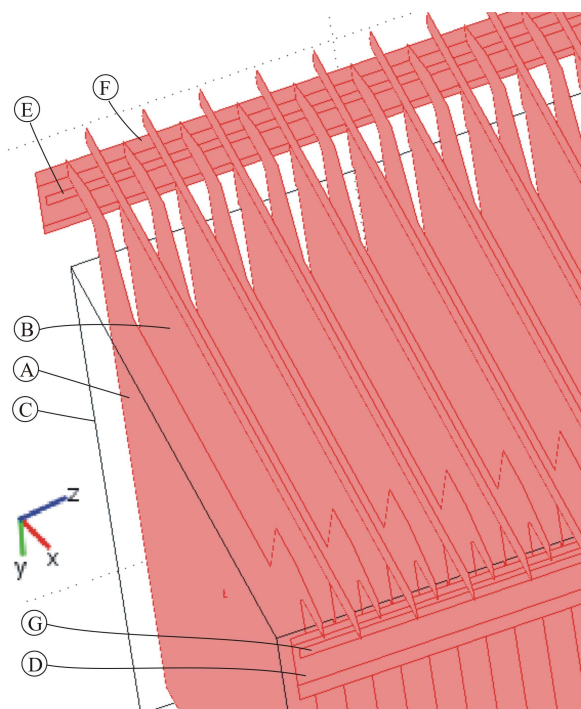


Fig. 4 The geometry of the ER cell FEM model

gle electrolysis cell model geometry shown in Fig. 4 contains solids, which increases the number of DOF. When expanding to the cell group model containing seven electrolysis cells, the necessary reduction in the number of DOF is achieved by shrinking the electrolyte and parts of electrodes in contact with electrolyte to the upper boundary of electrolyte. This is justified by the fact that the electrical potential in the electrode plate in contact with electrolyte is quite uniform. The resulting geometry of electrolysis cell group – containing only

shell elements – is depicted in Fig. 5. The geometry includes the anodes (A), the cathodes (B), the electrolyte (C) and the ICBB. The ICBB consist of the conductor segments (D) and the optional spacer segments (E). The spacer segments for the ICBB are disabled in Fig. 5.

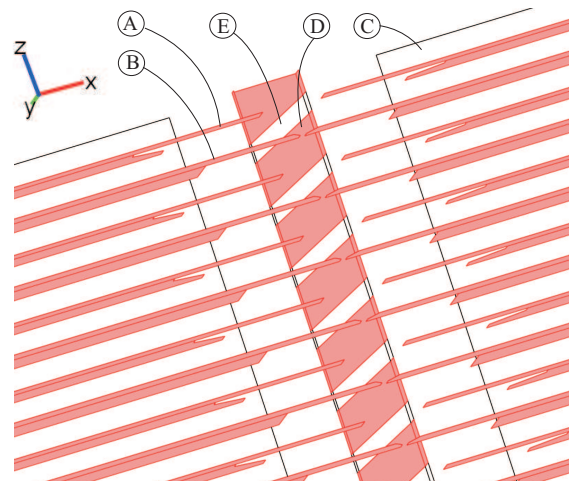


Fig. 5 A model geometry detail of the EW cell group with the fully split ICBB

Since the model geometry contains only shell elements and no solid objects, triangular elements can be used for the meshing. The choice of using points in the electrode busbar contacts causes singular sources into the model. This is a problem, since the solution depends strongly on the maximum element size used for the point [16, p. 497]. According to the process measurements, the electrode busbar contact is not considered to be singular in nature. Thus large element size is used to suppress the raise of dependent variables (e.g. electric potential and temperature) close to the contact point.

3.2 The empirical model of an electrode busbar contact

In the electrolysis cell FEM model [5] the electrode busbar contact resistance R_c is approximated by $R_c(T) = R_c^0 (1 + \alpha_c (T - T_c^0))$, where R_c^0 is the contact resistance at the reference temperature T_c^0 and α_c is the contact resistance temperature coefficient. The measurements suggest that such approximation is not very well justified. In the Fig. 6 the measurements of contact current are presented as function of the contact voltage drop. Measurements from distinct operating states – the cathode with and without short circuit – are annotated using different markers. As the contact current increases, both the variance and the growth rate of the voltage drop decrease.

In forming the empirical model of cathode contact only the centroids in Fig. 6 are used and the variance information is neglected. The cathode voltage drop is 40 mV at nominal current 650 A. The anode busbar contact voltage drop is assumed to be 15 mV in the ER and 35 mV in the EW at the same nominal current. The resulting empirical functions for the electrode busbar contact

currents are depicted in Fig. 7.

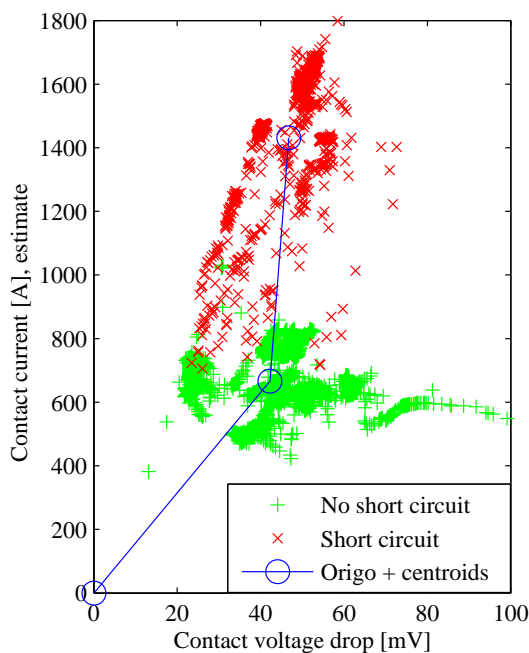


Fig. 6 The cathode busbar current as function of the contact voltage drop in the contact measurements

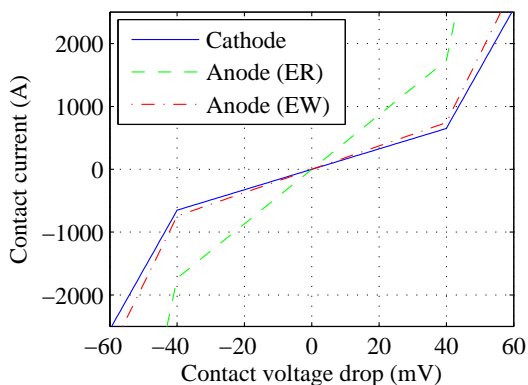


Fig. 7 The contact current for electrodes as function of the contact voltage drop in the contact empirical model

3.3 Electrical conduction

The shell elements are used to model the electrode geometries. Thus the gap between electrodes is changed compared to the real geometry. To maintain the desired cell voltage, the approximation of the electrical conductance $\tilde{\sigma}_e$ for the electrolyte is defined as

$$\tilde{\sigma}_e = \frac{\hat{I}_c}{(\hat{\mathcal{E}}_c - U_{ec}(\hat{I}_c))} \frac{D_a}{(A_a + A_c)}, \quad (5)$$

where \hat{I}_c is the nominal cathodic current, $\hat{\mathcal{E}}_c$ is a nominal cell voltage, U_{ec} is the voltage drop due to the electro-chemical reactions, D_a is spacing between adjacent anodes, A_a and A_c are the areas of one side of the

anode and cathode plates, that are in contact with the electrolyte. Laboratory measurements made by Outotec reveal that U_{ec} is function of the electrode current, or more generally, function of the electrode current density. The measurements indicate that U_{ec} it is about 0.05 V for the ER and about 1.6 V for the EW process when the current density is 100 – 400 A/m². In the modeling of the ER process cell group U_{ec} is neglected.

The constant supply current \hat{I}_s of electrolysis cell group is

$$\hat{I}_s = \hat{I}_c N_c, \quad (6)$$

where N_c is the number of cathodes in the electrolysis cell.

The electrical resistivity ρ for conductors is often formulated as $\rho(T) = \rho_0(1 + \alpha(T - T_0))$, where T is the temperature, ρ_0 is the resistivity at reference temperature T_0 and α is the temperature coefficient of resistivity. The electrical conductivity σ is given as a reciprocal of resistivity:

$$\sigma(T) = \frac{\sigma_0}{1 + \alpha(T - T_0)}, \quad (7)$$

where $\sigma_0 = 1/\rho_0$ is the electrical conductance at the reference temperature T_0 .

The current density $\mathbf{J} = \sigma \mathbf{E} = -\sigma \nabla U$, where \mathbf{E} is the electric field and U is the electric potential distribution. In the stationary case the electric potential distribution satisfies

$$\nabla \cdot \mathbf{J} = \nabla \cdot (-\sigma \nabla U) = 0. \quad (8)$$

When using the weak form modeling it is necessary to transform Eq. (8) into the weak form, which yields

$$\int_{\Omega} \sigma \nabla U \cdot \nabla U^t \, dV = 0, \quad (9)$$

where U^t is a test function for U and Ω is the domain. For the shell elements the thickness is taken into account by multiplying the integral in Eq. (9) by the thickness d and taking the integral over the shell element S , which yields

$$\int_S d \sigma \nabla U \cdot \nabla U^t \, dA = 0. \quad (10)$$

The cathode base plate is made of 3 mm thick acid proof steel. The part of the cathode plate in contact with the electrolyte is a composite structure in the model, since it is modeled to have 6.5 mm layer of copper deposit on both sides of the base plate. To approximate physical constants for such composite structure in the shell element modeling a weighted sum method is used, and the approximation for electrical conductivity $\tilde{\sigma}$ is thus

$$\tilde{\sigma} = \left(\sum_{i=1}^{N_m} A_i \right)^{-1} \sum_{i=1}^{N_m} \sigma_i A_i, \quad (11)$$

where N_m is the number of materials in composite structure, A_i is the cross sectional area and σ_i the electrical conductivity for the i th material.

The current supply of the cell group is modeled as uniform current density to the outermost cell busbar. This is implemented in the model by adding a weak contribution

$$\int_{L_s} -\frac{\hat{I}_s}{L_s} U^t ds \quad (12)$$

to the current supply line geometry, where L_s is the length of the current supply line geometry. The current sink is implemented in the model by adding a negation of Eq. (12) to the cathode busbar geometry on the other end of the cell group.

3.4 Heat transfer

For the heat transfer by conduction, the heat flux vector $\mathbf{q} = -k\nabla T$, where k is the thermal conductivity and T is the temperature field. In a stationary case, the temperature field satisfies

$$\nabla \cdot \mathbf{q} = \nabla \cdot (-k\nabla T) = Q, \quad (13)$$

where Q is the heat source. In a conductor, the heat source Q is resistive heating

$$Q = \frac{1}{\sigma} \|\mathbf{J}\|^2 = \sigma \|\nabla U\|^2. \quad (14)$$

Substituting Eq. (14) to Eq. (13) yields

$$\nabla \cdot (-k\nabla T) = \sigma \|\nabla U\|^2. \quad (15)$$

For composite structures, the thermal conductivity k is approximated similarly as in Eq. (11). According to the Eqs. (7) and (15) the electrical conduction and heat transfer are connected phenomena thus resulting in multiphysical model.

The natural boundary condition for heat transfer is modeled as convective flux q_{\perp} ,

$$q_{\perp} = \mathbf{n} \cdot \mathbf{q} = \bar{h}(T - T^{\infty}), \quad (16)$$

where \mathbf{n} is an outward unit normal vector for the surface, \bar{h} is the average heat transfer coefficient and T^{∞} is the ambient bulk temperature.

Transforming Eqs. (15) and (16) into the weak form for the shell element yields

$$\int_S \left[d(k\nabla T \cdot \nabla T^t - \sigma \|\nabla U\|^2 T^t) + \sum_{i=1}^2 q_{\perp,i} T^t \right] dA = 0, \quad (17)$$

where T^t is test function for T and $q_{\perp,i}$ is the convective heat flux

$$q_{\perp,i} = \bar{h}_i(T - T_i^{\infty}) \quad (18)$$

in the direction of outward-normal vector of the shell element. In Eq. (18) \bar{h}_i is the average heat transfer coefficient and T_i^{∞} the ambient bulk temperature associated for both surfaces of the shell element. Convection occurs also through the shell element boundaries

i.e. edges ∂S_j . This is managed by adding a weak contribution

$$\int_{\partial S_j} d\bar{h}_j(T - T_j^{\infty}) T^t ds \quad (19)$$

for each edge of the shell element.

The number of DOF for the proposed FEM model of the electrolysis cell group is about 75 000 for the electric potential and about 65 000 for the temperature. If shell elements are not used to simplify the model geometry, the number of DOF would be larger by several orders of magnitude. Besides, the COMSOL Multiphysics™ is not even able to create the default mesh for part of the single electrolysis cell containing only the electrolyte and the part of the electrodes in contact with the electrolyte.

4 Simulation results

The simulation results are presented only for the ER process and the short circuit disturbance. The simulated models are presented in Table 1. The ICBB is a sequence of fixed conductor segments and optional spacer segments. The fixed conductor segment connects the anode and the cathode of adjacent cells as depicted in Fig. 5. The optional spacer segment – if it exists – connects adjacent conductor segments in the ICBB to form longer segment. The ICBB configurations are presented in Fig. 8. A white rectangle indicates that the ICBB is split by removing the spacer segment. Particularly, all spacers exist for the Walker (Model 1) resulting in contiguous ICBB. The fully split Walker (Model 8) has only conductor segments and no spacers in the ICBB.

Tab. 1 Model configurations for the simulations

Model Id	Description	No. of ICBB conductor segments
1	Walker	1
2	ICBB split to 2 parts	2
3	ICBB split to 3 parts	3
4	ICBB split to 5 parts	5
5	ICBB split to 6 parts	6
6	ICBB split to 10 parts	10
7	ICBB split to 15 parts	15
8	Fully split Walker	31

4.1 The effective currents

In the copper industry, where usually only cathode current measurements are available, the current distribution evenness is measured as standard deviation of the cathodic current densities. The cathodic current density vector for the electrolysis cell is defined as $\mathbf{J}_c = \mathbf{I}_c / (2A_c)$, where $N \equiv N_c$ is shorthand notation for the number of cathodes in one cell, $\mathbf{I}_c = (c_1, c_2, \dots, c_N)^T$ is the vector of cathode currents and A_c half of the cathode plate area in contact with the electrolyte. In this paper the current distribution uniformity of the electrolysis cell group is defined as standard deviation of *effective currents*. The effective current is defined as the

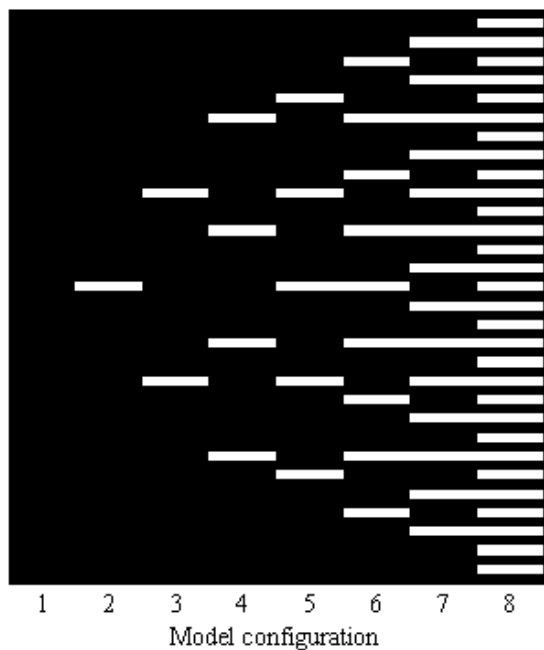


Fig. 8 The intercell busbar split patterns for the model configurations listed in Tab. 1

electric current through the electrolyte from the anode to the cathode and thus does not contain possible short circuit current.

The effective currents are computed from the electrode and the short circuit currents as follows. Let $\mathbf{I}_a = (a_1, a_2, \dots, a_{N+1})^T$ be the vector of anode currents of one electrolysis cell. The electrode gap currents \mathbf{I}_g are the electric currents from the anodes to the cathodes:

$$\mathbf{I}_g = \mathbf{I}_f + \mathbf{I}_s, \quad (20)$$

where \mathbf{I}_f are the effective currents and \mathbf{I}_s are the short circuit currents from the anodes to the cathodes, respectively. The electrode gap currents for one electrolysis cell can be solved from matrix equation

$$\mathbf{A}\mathbf{I}_g = \mathbf{I}_e, \quad (21)$$

where $\mathbf{I}_e = (a_1, c_1, \dots, a_N, c_N)^T$ is the vector of electrode currents and \mathbf{A} is the $2N \times 2N$ coefficient matrix. The coefficient matrix is a Toeplitz matrix having ones in main diagonal and 1st subdiagonal:

$$\mathbf{A} = \begin{pmatrix} 1 & 0 & 0 & \dots & 0 & 0 & 0 \\ 1 & 1 & 0 & \dots & 0 & 0 & 0 \\ 0 & 1 & 1 & \dots & 0 & 0 & 0 \\ \vdots & \vdots & \vdots & \ddots & \vdots & \vdots & \vdots \\ 0 & 0 & 0 & \dots & 1 & 0 & 0 \\ 0 & 0 & 0 & \dots & 1 & 1 & 0 \\ 0 & 0 & 0 & \dots & 0 & 1 & 1 \end{pmatrix} \quad (22)$$

Using Eqs. (20), (21) and (22), the effective current matrix \mathbf{l}_f for the N_g cell electrolysis cell group can be solved from matrix equation

$$\mathbf{l}_f = \mathbf{A}^{-1}\mathbf{l}_e - \mathbf{l}_s, \quad (23)$$

where matrices \mathbf{l}_f , \mathbf{l}_e and \mathbf{l}_s contain vectors \mathbf{I}_f , \mathbf{I}_e and \mathbf{I}_s for each of the N_g electrolysis cells as their columns, respectively. The Eq. (23) is solved in the MATLAB[®] effectively using the backslash operator: $\mathbf{l}_f = \mathbf{A} \setminus \mathbf{l}_e - \mathbf{l}_s$.

In the copper industry it is difficult to measure the effective currents in real-time because the short circuit currents are needed in the calculation. However, the time average of the effective current could be estimated by measuring the copper deposit separately from each side of the cathode plate.

4.2 The effect of disturbance location

The effect of short circuit location on the short circuit current and the cell group voltage is depicted in Figs. 9 and 10. The location of the short circuit is changed over each electrode gap in the midmost cell of the cell group. Simulation results from only three of the eight model configurations are presented. The change in the performance measures is small in the Walker System because the elongated ICBB allows the electric current to flow in the direction of the cell. When the ICBB is split into six parts the short circuit current drops significantly as the short circuit is at the segment boundary. At the same time the cell group voltage increases somewhat. For the fully split Walker the short circuit current decreases and the cell group voltage increases compared to the other model configurations. In addition, the variation in the performance measures increases significantly when the short circuit is located close to the end of the electrolysis cell.

4.3 Comparison of the ICBB systems

To eliminate the effect of the short circuit location on the performance measures the statistical approach is used. The location of short circuit is assumed to be uniformly distributed, so that the averages of the short circuit current and the cell voltage over all short circuit locations can be used.

Let $\text{msum}(\mathbf{A})$ be the sum of elements of $M \times N$ matrix \mathbf{A} ,

$$\text{msum}(\mathbf{A}) = \sum_{j=1}^N \sum_{i=1}^M a_{ij}. \quad (24)$$

Since the supply current \hat{I}_s passes through each electrolysis cell in the cell group in the simulations,

$$\text{msum}(\mathbf{I}_g) = \hat{I}_s \quad (25)$$

and

$$\text{msum}(\mathbf{l}_g) = N_g \hat{I}_s. \quad (26)$$

The current efficiency η_I^g of the cell group is calculated in the simulations as

$$\eta_I^g = \frac{\text{msum}(\mathbf{l}_f)}{\text{msum}(\mathbf{l}_g)} = \frac{\text{msum}(\mathbf{l}_f)}{N_g \hat{I}_s}, \quad (27)$$

where Eqs. (2), (3) and (26) have been used. However, the current efficiency is 100 % for all cells except the

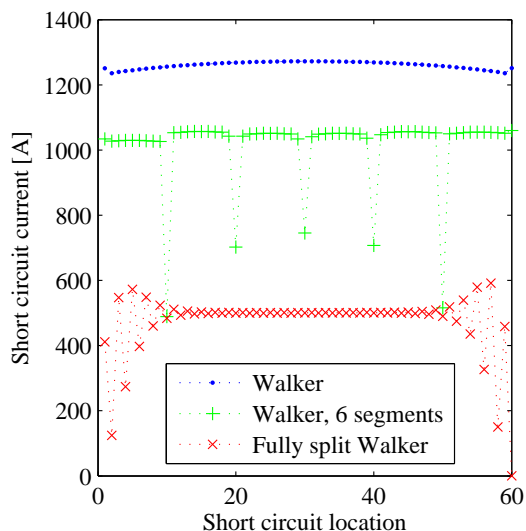


Fig. 9 The short circuit current vs. the short circuit location

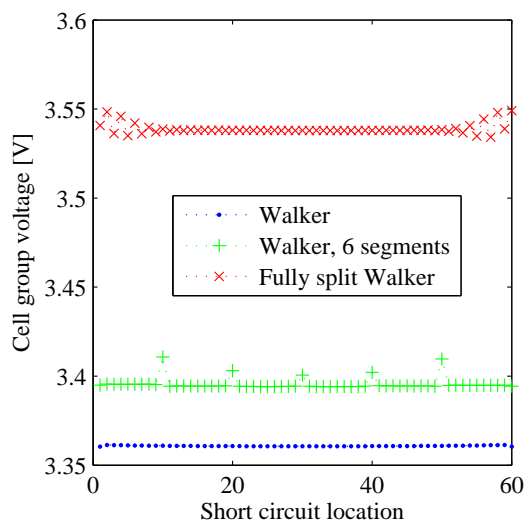


Fig. 10 The cell group voltage vs. the short circuit location

midmost cell, which have current loss due to the short circuit. The current efficiency η_l^c for the midmost cell is calculated in the simulations as

$$\eta_l^c = \frac{\text{msum}(\mathbf{I}_f)}{\text{msum}(\mathbf{I}_g)} = \frac{\text{msum}(\mathbf{I}_f)}{\hat{I}_s}, \quad (28)$$

where \mathbf{I}_f and \mathbf{I}_g are calculated for the midmost cell.

It is meaningful to calculate the current efficiency for the single cell. However, the specific energy consumption should be calculated for the cell group because both the model configuration and the presence of the short circuit may change the current distribution of the whole cell group. In the stationary case the electric energy consumption in Eq. (4) is

$$E_e = \mathcal{E}_s \hat{I}_s t_p, \quad (29)$$

where \mathcal{E}_s is the voltage drop in the cell group and t_p is

the production time. Accordingly, using Eq. (2), the produced cathode copper is

$$m_{\text{cu}} = \zeta_{\text{cu}} \text{msum}(\mathbf{I}_f) t_p. \quad (30)$$

Finally, using Eqs. (4), (27), (29) and (30), the specific energy consumption of the cell group is calculated in the simulations as

$$E_s = \frac{E_e}{m_{\text{cu}}} = \frac{1}{\zeta_{\text{cu}}} \frac{\bar{\mathcal{E}}_c}{\eta_l^g}, \quad (31)$$

where $\bar{\mathcal{E}}_c = \mathcal{E}_s / N_g$ is the average cell voltage of the cell group.

The results of the statistical approach are presented in Figs. 11 and 12 together with the result when the short circuit is in the middle of the cell (short circuit location is 30). When the performance measures are evaluated for the fixed short circuit location, the short circuit current as function of the standard deviation of effective currents behaves quite irregularly (see Fig. 11). The statistical approach indicates that the current efficiency as well as the deviation of the effective currents increase monotonically as the number of the ICBB segments increases.

Both the results calculated using the fixed short circuit location and the statistical approach indicate that the specific energy consumption (c.f. Fig. 12) increases monotonically as the number of ICBB segments increases.

5 Conclusions

A multiphysical FEM model of the copper electrolysis cell group together with the empirical model of electrode busbar contact is presented. A new concept – the effective current – is introduced for measuring the current uniformity of the cell group. Simulations are used to evaluate the effect of the location of short circuit on the performance of the electrolysis cell group. A statistical approach is proposed to eliminate the effect of short circuit location on the performance measures so that the effect of the ICBB splitting can be estimated.

The FEM model is computationally feasible. In addition, it is more accurate than resistance networks, which have been used in the past for modeling copper electrolysis cell group. The proposed model can be further improved for example by introducing time dependent and stochastic phenomena into the model.

The use of effective currents in measuring the uniformity of current density is well justified in the simulations but it requires measurements of short circuit currents, which are not directly measurable in the copper industry.

The simulation results reveal that the splitting of the ICBB has significant effect on the performance of the electrolysis cell group. Moreover, the statistical approach used in this paper clarifies the effects of the ICBB splitting on the performance measures of the electrolysis cell group.

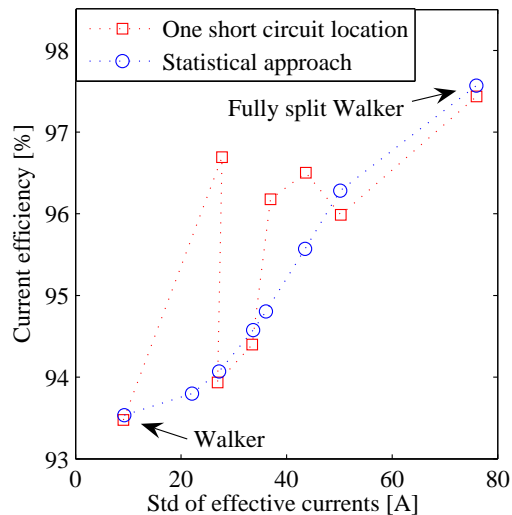


Fig. 11 The current efficiency vs. the standard deviation of the effective currents in the midmost electrolysis cell in the cell group

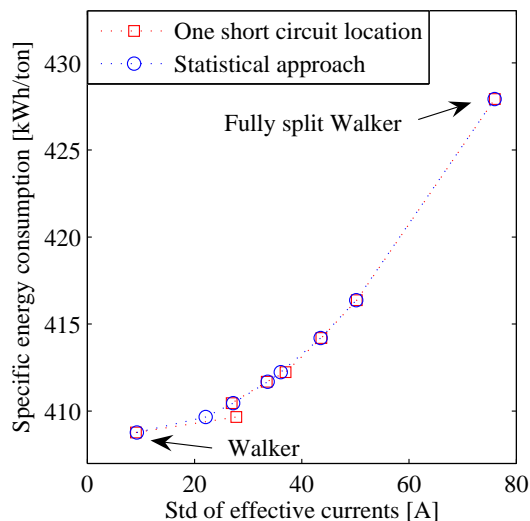


Fig. 12 The specific energy consumption vs. the standard deviation of the effective currents

6 Acknowledgements

We would like to thank MSc. Timo Kumara from Outotec Oyj for the cathode contact measurements and Dr. Reijo Laihia from Tampere University of Technology for his contributions. The financial support from the Finnish Funding Agency for Technology and Innovation (TEKES) (project MASIY52), Outotec Oyj and the Satakunta Korkeakoulu Foundation (Satakunnan Korkeakoulusäätiö) is gratefully acknowledged.

7 References

- [1] W.G. Davenport, M. King, M. Schlesinger, and A.K. Biswas. *Extractive metallurgy of copper – 4th ed.* Elsevier Science Ltd., Oxford, 2002.
- [2] E.P. Wiechmann, G.A. Vidal, and A.J. Pagliero. Current-source connection of electrolytic cell

electrodes: An improvement for electrowinning and electrorefining. In *IEEE transactions on industry applications*, vol. 42, no. 3, pages 851–855. IEEE Transactions, Jan 26 2006.

- [3] I.S. Laitinen, H.K. Virtanen, O.T. Järvinen, T.M. Kumara, and J.T. Tantt. Finite element modeling of an electrolysis cell. In *Accepted to be presented in Cu2007 the 6th Copper/Cobre Conference*, Toronto, Aug 25-30 2007.
- [4] G.A. Vidal, E.P. Wiechmann, and A.J. Pagliero. Technological improvements in copper electrometallurgy: Optibar segmented intercell bars (patent pending). In *Canadian Metallurgical Quarterly*, Vol. 44, No 2, pages 147–154. Canadian Institute of Mining, Metallurgy and Petroleum, Apr 2005.
- [5] I.S. Laitinen and J.T. Tantt. FEM modeling of an industrial scale electrolysis cell. In Lars Gregersen, editor, *Nordic Comsol Conference 2006, Copenhagen*, pages 29–34. Comsol, Nov 1 2006.
- [6] A.L. Walker. Plant for the electrodeposition of metals, United States Patent No. 6878003. Dec 3 1901.
- [7] R.L. Whitehead. Electrolytic apparatus, United States Patent No. 1206965. Dec 5 1916.
- [8] H. Virtanen, T. Marttila, and R. Pariani. Outokumpu moves forward towards full control and automation of all aspects of copper refining. In *Proceedings of the Copper 99 – Cobre 99*, pages 207–225, Phoenix, Arizona, USA, Oct 10-13 1999.
- [9] H. Virtanen, I. Virtanen, T. Kivistö, and T. Marttila. Busbar construction for electrolytic cell, United States Patent No. 6342136. Jan 2002.
- [10] T. Marttila, L. Palmu, and H. Virtanen. Advanced tankhouse systems by Outokumpu. In *Copper 2003 / Cobre 2003*, vol. V, Santiago, Chile, pages 121–135, 2003.
- [11] A.K. Biswas and W.G. Davenport. *Extractive metallurgy of copper – 1st ed.* Pergamon Press, 1976.
- [12] R. Serway, C. Moses, and C. Moyer. *Modern Physics*, 3th ed. 2005.
- [13] COMSOL *Multiphysics User's Guide*. COMSOL AB, 2005.
- [14] R.C. McOwen. *Partial Differential Equations: Methods and Applications*, 2nd ed. Prentice Hall, Upper Saddle River, 2003.
- [15] COMSOL *Multiphysics Modeling Guide*. COMSOL AB, 2005.
- [16] K.H. Huebner, D.L. Dewhirst, D.E. Smith, and T.G. Byrom. *The Finite Element Method for Engineers*. John Wiley & Sons, Inc., New York, 2001.